Araştırma Makalesi https://doi.org/10.46810/tdfd.1097511 Research Article

Türk Doğa ve Fen Dergisi
Turkish Journal of Nature and Science
www.dergipark.gov.tr/tdfd

# Evaluation of Mechanical Performance of a Fe-Mn-Si Biodegradable Stent using Finite Element Simulations

**Nazim BABACAN**[1*]

[1] Sivas Bilim ve Teknoloji Üniversitesi, Mühendislik ve Doğa Bilimleri Fakültesi, Makine Mühendisliği Bölümü, Sivas, Türkiye
Nazim BABACAN ORCID No: 0000-0003-2173-8656

**Corresponding author: nazimbabacan@sivas.edu.tr*

(Received: 02.04.2022, Accepted: 14.06.2022, Online Publication: 29.06.2022)

**Keywords**
Biodegradable Stent, Fe–Mn–Si Shape Memory Alloy, Finite Element Analysis, Mechanical Performance

**Abstract:** Biodegradable metal stents are potential stent candidates as they dissolve in the body over time after fulfilling their mechanical duties and therefore do not pose a risk in the future. Fe-30Mn-6Si biodegradable alloy was found to be successful in the previous studies in terms of mechanical strength and biodegradability. In this study, the expansion and recoiling behavior of a stent made of Fe-30Mn-6Si alloy was investigated using finite element analyses. L605 Co-Cr and 316L stainless steel stents were also examined for comparison. Obtained results showed that novel FeMnSi stent exhibits lower equivalent stress than the counterparts. On the other hand, the lowest equivalent plastic strain and the highest radial elastic recoil value were observed in FeMnSi stent. Overall findings indicate that FeMnSi stent is moderately successful in terms of balloon-stent interaction.



# Fe-Mn-Si Biyobozunur Stentlerin Mekanik Performansının Sonlu Eleman Simülasyonları Kullanılarak Değerlendirilmesi

**Anahtar Kelimeler**
Biyobozunur stent, Fe-Mn-Si Şekil Hafızalı Alaşım, Sonlu Eleman Analizi, Mekanik performans

**Öz:** Biyobozunur metal stentler, mekanik görevlerini yerine getirdikten sonra zamanla vücut içerisinde çözüldükleri ve bu nedenle gelecekte bir risk oluşturmadıkları için potansiyel stent adaylarıdır. Önceki çalışmalarda, Fe-30Mn-6Si biyobozunur alaşımı mekanik dayanım ve biyolojik olarak parçalanabilirlik açısından başarılı olduğu görülmüştür. Bu çalışmada, Fe-30Mn-6Si alaşımından yapılmış bir stentin genleşme ve geri tepme davranışı sonlu eleman analizleri kullanılarak incelenmiştir. Karşılaştırma için L605 Co-Cr ve 316L paslanmaz çelik stentler de incelenmiştir. Elde edilen sonuçlar, yeni FeMnSi stentinin muadillerine göre daha düşük eşdeğer gerilme sergilediğini göstermiştir. Öte yandan, en düşük eşdeğer plastik gerinim ve en yüksek radyal elastik geri tepme değeri FeMnSi stentte gözlenmiştir. Genel bulgular, FeMnSi stentin balon-stent etkileşimi bakımından orta düzeyde başarılı olduğunu göstermektedir.

## 1. INTRODUCTION

Stents are used to open up coronary artery blockages by providing a structural support. These meshed tubes are often deployed by a balloon which is expanded with a pressure and placed inside the diseased region of the artery. Large plasticity is required for a balloon-expandable stent material to minimize the elastic recoiling effect when it is released in the vessel [1]. Co-Cr based and 316L stainless steel are among the most frequently used metal stent alloys owing to high strength, plasticity and biocompatibility [2, 3].

In recent years, as alternative to these permanent stents, biodegradable stents, that are resolved after providing scaffolding and therefore, no need to further usage after the healing is completed, have been developing by the scientists [4-6]. These new-generation stent type does not allow long-term complications, such as chronic inflammation, and physical irritation caused by the usage of permeant stents and thus, prevent the possible secondary surgeries for stent removal [7, 8]. Among the metal biodegradable stents, Mg-based, Zn-based and Fe-based alloys are seen as the most popular ones. Due to the relatively higher strength and lower degradation rate, Fe-based alloys have several advantages over their counterparts, such as using thinner strut thickness and

maintaining mechanical integrity for a longer period of time [9-11].

In the recent studies, Fe-(28-30)Mn-(5-6)Si (wt%) shape memory alloys were seen as a potential biodegradable stent candidate as a result of some corrosion and mechanical tests [12-15] and thus, it would be useful to investigate its mechanical response when it is inflated by the balloon by comparing with the performance of other reference stent materials.

One of the efficient methods to study and investigate the mechanical behavior of the stents without performing expensive tests is finite element (FE) analysis [16]. Stress evaluation and the determining the critical regions over the entire part are also possible in this method which are quite beneficial for designing. Many researchers investigated the mechanical performance of the stents by examining the effect of different parameters such as strut geometries, material properties and radial pressure were investigated by utilizing from FE methods [17-19].

In this study, it is aimed to examine the mechanical performance of a Fe-30Mn-6Si stent involving the deployment and recoiling stages by FE simulations. Equivalent stress and plastic strain values during these steps as well as recoiling ratio for this stent material were obtained and these values were compared with those of Co-Cr based and 316L stainless steel stents for better evaluation.

## 2. MATERIAL AND METHODS

### 2.1. Finite Element Model

Solid model of the stent was generated by SolidWorks software. 2D sketch was wrapped around a cylinder whose diameter equals to the stent diameter in order to create 3D model. The diameter and the length of the stent are 4.07 and 15.72 mm, respectively. Strut thickness was chosen as 60 µm. 3D model and the 2D sketch of a single unit are seen in Figure 1. The length of the bridge that connects the single units is 0.76 mm.

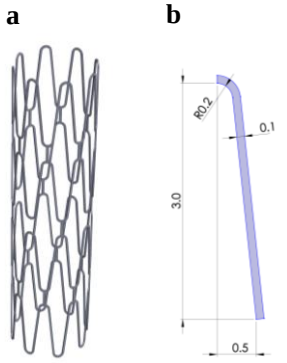


**Figure 1.** (a) Final 3D model of the stent, (b) Sketch for the single repeating unit of the design

A shell balloon element with a diameter of 3.85 mm and a thickness of 4 µm was added to the model. Since the stent geometry is symmetrical, 1/8 symmetry of the whole model was used to minimize the computational cost caused by excessive number of elements. FE model created by Ansys/Static Structural program is shown in Figure 2. The mesh of the stent was generated by hexagon dominant multizone method by defining the element size of 0.015 mm. Quadrilateral shell elements was used to create the balloon model and element size was chosen as 0.05 mm. The model consists of a total 65236 elements.

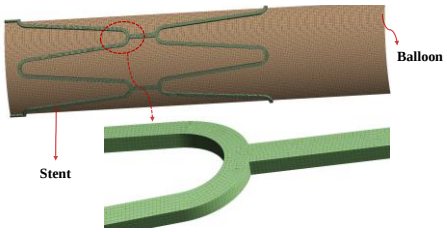


**Figure 2.** 1/8 symmetric finite element (FE) model. (A portion of the stent is magnified in the below to better view the FE mesh.)

A surface to surface frictionless contact between the interior surface of the stent and the exterior surface of the balloon was defined. Frictionless supports were applied from the surfaces as shown in Figure 3 as symmetry boundary conditions. 1 mm radial displacement was applied from the balloon surface as a loading and then, subsequently balloon was retracted to initial position.

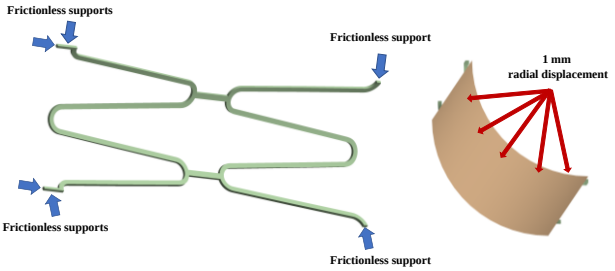


**Figure 3.** Applied boundary conditions in the FE model.

### 2.1. Material Properties

The balloon was assigned a Mooney-Rivlin hyperelastic material property. C10 and C01 material constants of Mooney-Rivlin 2 Parameter were defined as 1.06 and 0.114 MPa [20]. Multilinear isotropic hardening material model was used to define stent behaviors. While Mooney-Rivlin hyperelastic material model is suitable for materials that deform substantially elastically, multilinear isotropic hardening material model is very useful for alloys whose stress-strain data are obtained with experimental methods since it uses the plastic strain/yield stress points as data input. Stent material was chosen as Fe-30Mn-6Si, L605 Co-Cr and 316L stainless steel alloys in three different analyses. True stress-strain graphs in the literature (see Figure 4) were utilized to determine plastic strain-stress values and the material properties of the used alloys are shown in Table 1.

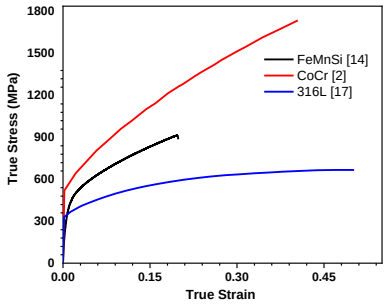


**Figure 4.** True stress-strain graphs adapted from literature to model Fe-30Mn-6Si, L605 Co-Cr and 316L stainless steel alloys

**Table 1**. Material properties of the alloys used as a stent material

| | FeMnSi [14] | L605 Co-Cr [2] | 316L [21] |
|---|---|---|---|
| **Young's Modulus (GPa)** | 120 | 240 | 201 |
| **Poisson's ratio** | 0.3 | 0.3 | 0.3 |
| **Yield Stress (MPa)** | 266 | 520 | 330 |

## 3. RESULTS AND DISCUSSION

### 3.1. Equivalent Stress Distribution

Von Mises (equivalent) stress distribution of three different stents, that are made of Fe-30Mn-6Si, L605 Co-Cr and 316L, after 1 mm radial displacement and springback stages are shown in Figure 5. Stress distributions seem to be independent from the material of the stent. While the maximum stress values are observed in Co-Cr stent, the minimum values are in FeMnSi stent both after loading and unloading. Stress concentrations occurred on the top and bottom surfaces of the crown radius parts after loading as seen in Figure 5(a, c and e). However, after unloading, i.e. after removing the balloon, there is no prominent stress values at the large portion of the stents and stress concentrations are seen in a very small region on the front and back side of the crown radius parts as exemplified by a highlighted image in Figure 5(b).

The stress values and distribution during the implantation of a stent is a critical parameter for a stent design. High stress that occurs in a large cross-section can be serious and the stent would fail. FeMnSi and 316L stents (as observed in Figure 5(a and c)) show lower stress values compared to Co-Cr stent. However, it should be noted that strength of Co-Cr alloy is relatively high and stress values do not exceed its ultimate tensile limit. Moreover, residual stress values at the outer surfaces of the stents are also important since high values can trigger corrosion [4, 22]. Therefore, low residual stress values seen in FeMnSi stent compared to its counterparts could be an advantage for it. Even though, biodegradable FeMnSi stent is desired to degrade by time, corrosion induced by stress concentration causes a non-homogenous degradation and breaks the integrity of the stent.



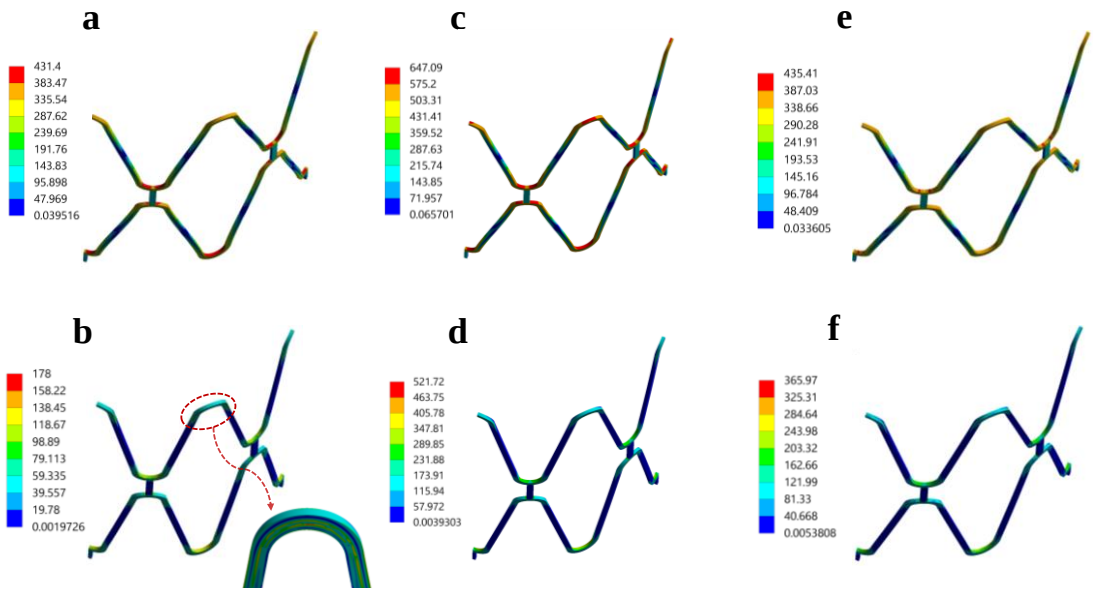


**Figure 5.** Equivalent stress distribution of (a, b) of Fe-30Mn-6Si, (c, d) L605 Co-Cr and (e, f) 316L stainless steel stents (a, c, e) after 1 mm radial displacement (b, d, f) after springback

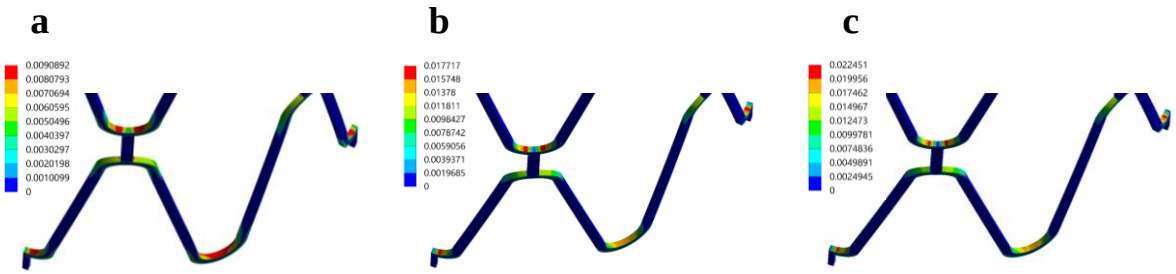


**Figure 6.** Equivalent plastic strain distribution of (a) Fe-30Mn-6Si, (b) L605 Co-Cr and (c) 316L stainless steel stents after 1 mm radial displacement

### 3.2. Equivalent Plastic Strain and Elastic Recoil

The equivalent plastic strains occurred after 1 mm radial deformation are presented in Figure 6 for all three stents. Since the plastic strains did not change after the expansion recoil, those results were not added. Plastification is found at the same regions where high stress values as seen in Figure 5(a, c and e). The highest plastic strains occurred in 316L stainless steel stent with a maximum value of 0.0224 mm/mm. Whereas, the maximum values of Co-Cr and FeMnSi stents are 0.0177 and 0.0091 mm/mm, respectively. Low elastic modulus value and the late onset of the plastic deformation in the FeMnSi stent resulted a lower plastic strain compared to other stents.

Plastic strains observed in the stents also influence the radial elastic recoil (ER) responses. Radial ER values were calculated and tabulated in Table 2 for each stent model by utilizing the FE results according to ASTM F2079-09 [23] as in Equation 1:

$$Radial\ ER = \frac{R_{load} - R_{unload}}{R_{load}}\ x\ 100\% \qquad (1)$$

where $R_{load}$ and $R_{unload}$ are the radius of the stent after the expansion and springback, respectively.

**Table 2**. Radial elastic recoil values for the analyzed stents

| Fe-30Mn-6Si | L605 Co-Cr | 316L |
|---|---|---|
| 17.05 % | 14.29 % | 10.90 % |

The highest elastic recoil value was obtained in the FeMnSi stent. It means that FeMnSi stent recovers more compared to other stents during the unloading and this behavior shows the higher flexibility of FeMnSi stent. Low plastic strain values seen in this stent is also related with the high elastic recoil behavior since these two responses have an opposite trend. Generally, a high value of elastic recoil is unfavorable for stent designs as the stent will not be exactly in the desired diameter in the final situation. However, there is no big difference between the degree of radial ER of the currently available L605 Co-Cr and potential Fe-30Mn-6Si stents. It should be mentioned that the radial ER values obtained in this study are higher than the design criteria (ER<4% [24]) of the stents. Nonetheless, a high value of expansion was applied in this study to see the mechanical strengths of the stents under extreme deformation and thus, higher radial ER values were obtained than the constraints. Therefore, it would be more sense to compare the ER values among the different stent materials not focusing the quantitative values.

## 4. CONCLUSIONS

In this study, mechanical response of the Fe-30Mn-6Si balloon expandable stent after the expansion and recoiling was investigated by using FE analyzes. The obtained equivalent stress and plastic deformation results as well as radial elastic recoil values for this stent were compared with those of L605 Co-Cr and 316L stainless steel stents.

The findings showed that lower stress values occurred in FeMnSi and 316L stents compared to Co-Cr stent. The lowest residual stress was seen in FeMnSi stent after recoiling which could be beneficial for the novel design due to the reduced risk of stress-induced corrosion. Owing to the lowest Young's modulus value and highest elasticity FeMnSi stent showed the lowest plastic strain and the highest radial elastic recoil compared to other stents. However, radial elastic recoil of the FeMnSi stent was found to be close to L605 Co-Cr stent. As a conclusion, the mechanical response of FeMnSi biodegradable stent was found to be promising by considering the balloon-stent interaction.

## REFERENCES

[1] Debusschere N, Segers P, Dubruel P, Verhegghe B, Beule M De. A finite element strategy to investigate the free expansion behaviour of a biodegradable polymeric stent. J Biomech. 2018;48(10):2012–8.

[2] Kumar A, Bhatnagar N. Finite element simulation and testing of cobalt-chromium stent: a parametric study on radial strength, recoil, foreshortening, and dogboning. Comput Methods Biomech Biomed Engin. 2021;24(3):245–59.

[3] Wang H, Wang X, Qian H, Lou D, Song M, Zhao X. The optimal structural analysis of cobalt-chromium alloy (L-605) coronary stents. Comput Methods Biomech Biomed Engin. 2021;24(14):1566–77.

[4] Galvin E, Brien DO, Cummins C, Donald BJ Mac, Lally C. A strain-mediated corrosion model for bioabsorbable metallic stents. Acta Biomater. 2017;55:505–17.

[5] Gu X, Mao Z, Ye SH, Koo Y, Yun Y, Tiasha TR, et al. Biodegradable, elastomeric coatings with controlled anti-proliferative agent release for magnesium-based cardiovascular stents. Colloids Surfaces B Biointerfaces. 2016;144:170–9.

[6] Xu C, Yin Z, Roy-Chaudhury P, Campos-Naciff B, Hou G, Schulz M. The development of a magnesium biodegradable stent: design, analysis, fabrication, and in-vivo test. Med Res Arch. 2020;8(9).

[7] Schinhammer M, Hänzi AC, Löffler JF, Uggowitzer PJ. Design strategy for biodegradable Fe-based alloys for medical applications. Acta Biomater. 2010;6(5):1705–13.

[8] Feng YP, Gaztelumendi N, Fornell J, Zhang HY, Solsona P, Baró MD, et al. Mechanical properties, corrosion performance and cell viability studies on newly developed porous Fe-Mn-Si-Pd alloys. J Alloys Compd. 2017;724:1046–56.

[9] Loffredo S, Paternoster C, Giguère N, Barucca G, Vedani M, Mantovani D. The addition of silver affects the deformation mechanism of a twinning-induced plasticity steel: Potential for thinner degradable stents. Acta Biomater. 2019;98:103–13.

[10] He J, He FL, Li DW, Liu YL, Liu YY, Ye YJ, et al. Advances in Fe-based biodegradable metallic materials. RSC Adv. 2016;6(114):112819–38.
[11] Donik Č, Kocijan A, Paulin I, Hočevar M, Gregorčič P, Godec M. Improved biodegradability of Fe–Mn alloy after modification of surface chemistry and topography by a laser ablation. Appl Surf Sci. 2018;453(March):383–93.
[12] Liu B, Zheng YF, Ruan L. In vitro investigation of Fe30Mn6Si shape memory alloy as potential biodegradable metallic material. Mater Lett. 2011;65(3):540–3.
[13] Drevet R, Zhukova Y, Malikova P, Dubinskiy S, Korotitskiy A, Pustov Y, et al. Martensitic Transformations and Mechanical and Corrosion Properties of Fe-Mn-Si Alloys for Biodegradable Medical Implants. Metall Mater Trans A. 2018;49(3):1006–13.
[14] Babacan N, Kochta F, Hoffmann V, Gemming T, Kühn U, Giebeler L, et al. Effect of silver additions on the microstructure, mechanical properties and corrosion behavior of biodegradable Fe-30Mn-6Si. Mater Today Commun. 2021;28(July):102689.
[15] Babacan N. Shape memory characteristics of silver-added Fe – 30Mn – 6Si Alloy. Trans Indian Inst Met. 2022;.
[16] Azaouzi M, Makradi A, Belouettar S. Numerical investigations of the structural behavior of a balloon expandable stent design using finite element method. Comput Mater Sci. 2013;72:54–61.
[17] Chen C, Xiong Y, Jiang W, Wang Y, Wang Z, Chen Y. Experimental and numerical simulation of biodegradable stents with different strut geometries. Cardiovasc Eng Technol. 2020;11(1):36–46.
[18] Kumar A, Bhatnagar N. Finite element simulation and testing of cobalt-chromium stent: a parametric study on radial strength, recoil, foreshortening, and dogboning. Comput Methods Biomech Biomed Engin. 2021;24(3):245–59.
[19] Britto JJJ, Venkatesh R, Prabhakaran R, Amudhan K. Design optimization of biomedical stent under the influence of the radial pressure using FEM. Mater Today Proc. 2021;39:1332–6.
[20] Cornell simulation YouTube channel [Internet] [cited 2022 May 20]. Available from: https://www.youtube.com/channel/UC8bXUXdcNDyFTIp6YVrtReg.
[21] Kim D-Y, Lee S-Y, Kim H-Y. Numerical evaluation and shape design of coronary artery stent. J Korean Soc Precis Eng. 2012;29(1):103–8.
[22] Chen Y, Shang X. Investigation on large elastoplastic deformation in expansion and springback for a composited bioresorbable stent. J Mech Behav Biomed Mater. 2021;119(February):104500.
[23] ASTM F2079-09(2017), Standard Test Method for Measuring Intrinsic Elastic Recoil of Balloon-Expandable Stents; ASTM International: West Conshohocken, PA, USA, 2017.
[24] Bowen PK, Drelich J, Goldman J. Zinc exhibits ideal physiological corrosion behavior for bioabsorbable stents. Adv Mater. 2013;25(18):2577–82.